

Molecular bipolar outflow in SN 1987A supports the jittering-jets explosion mechanism

NOAM SOKER¹

¹*Department of Physics, Technion - Israel Institute of Technology, Haifa, 3200003, Israel; soker@technion.ac.il*

ABSTRACT

I examine high-quality CO and SiO molecular maps of the core-collapse supernova (CCSN) remnant SN 1987A from the literature and find that the molecular gas exhibits a bipolar structure, correlated with the visible bipolar morphology (termed the keyhole) and the bipolar morphology of the iron emission map. The keyhole has a morphology similar to that of many jet-shaped pairs of bubbles in cooling-flow clusters of galaxies and planetary nebulae. Therefore, the findings of this study, which make the bipolar structure of SN 1987A robust, strengthen the claim that a pair of energetic jets shaped the keyhole and its surroundings. According to the jittering-jets explosion mechanism (JJEM), this pair of jets was the most energetic of several pairs that exploded SN 1987A. This study adds to the accumulating evidence that the JJEM is the primary explosion mechanism of CCSNe, responsible for the majority, or even all, CCSNe.

1. INTRODUCTION

The iconic core-collapse supernova (CCSN), now a CCSN remnant (CCSNR), SN 1987A, is one of the ‘battlegrounds’ between the two competing theoretical explosion mechanisms that aim to explain CCSNe: the jittering-jet explosion mechanism (JJEM; Soker 2024a, 2025a for recent reviews and Shiran & Soker 2025; Soker 2026a; Wang et al. 2025 for recent papers) and the neutrino-driven mechanism (the delayed neutrino mechanism; e.g., Janka 2025a,b for recent reviews and Giudici et al. 2025; Luo et al. 2026; Murphy et al. 2025; Orlando 2026; Rusakov et al. 2026; Varma & Müller 2026 for some recent papers). The observables during the explosion, such as the neutrino emission and explosion energy of SN 1987A, cannot distinguish between the two theoretical explosion mechanisms (e.g., Soker 2025a). Therefore, studies of the two explosion mechanisms compare the structure of SN 1987A ejecta with their predictions.

Some studies have argued that the neutrino-driven mechanism can explain the basic structural properties of SN 1987A (e.g., Janka et al. 2017; Alp et al. 2019; Jerkstrand et al. 2020; Gabler et al. 2021). Some find that the neutrino-driven mechanism can explain some, but not all, properties of SN 1987A, e.g., McCray & Fransson (2016), referring to Utrobin et al. (2015) and Wongwathanarat et al. (2015). In Soker (2017), I compared a three-dimensional (3D) iron structure of SN 1987A from Larsson et al. (2016) with 3D simulations of the neutrino-driven mechanism from Wongwathanarat et al. (2015), and found that they disagree; I argued for the JJEM. Later papers in the framework of the JJEM that

studied SN 1987A found that the JJEM can explain the large-scale morphology of SN 1987A (Bear & Soker 2018; Soker 2024b,c). Most recently, in Soker (2025b) I referred to new observations of SN 1987A (e.g., Bouchet et al. 2024; Matsuura et al. 2024), and strengthened the claim for a bipolar structure in relation to the dust distribution. Some more recent simulations also highlight the need for a bipolar explosion in SN 1987A (e.g., Ono et al. 2020; Orlando et al. 2020, 2025).

In a recent study, Wesson et al. (2026) compared the 3D structure of SN 1987A with 3D simulations within the framework of the neutrino-driven mechanism and argued for some similarities, although their simulations could not account for all of SN 1987A’s morphological properties. I find the agreement between the simulations and the 3D structure of SN 1987A poor. To compare the SiO and CO ALMA observations with the simulations, they generated intensity maps with a minimum intensity threshold of twice the noise threshold. In Section 2, I use their new observational images with the outer regions, as well as earlier ones, to identify outflow components in SN 1987A. In Section 3, I show that these outflow components fit the bipolar structure of SN 1987A, the ‘keyhole.’ In Section 4, I argue that this structure is compatible with the JJEM.

2. OUTFLOW COMPONENTS

2.1. Iron components

In this section, I identify outflow components that I relate to the bipolar structure of SN 1987A in Section 3. Towards that goal, I start with a set of Doppler maps from Larsson et al. (2023) that I present in Figure 1.

I identify four bright, distinguishable outflow components; I point to the tips of each. Two are bright regions, FeNB and FeS0, while two are much fainter, FeNR and FeSR; ‘Fe’ indicates that the components are identified in the [Fe I] 1.443 μm line, ‘N’ and ‘S’ mark north and south, respectively, and the last letter indicates whether the component is blueshifted, redshifted, or has about zero Doppler shift.

Component FeNB is a highly blueshifted component prominent in the $[-2000, -1000]$ km s^{-1} range. The red line indicates that this component points north (up) in these images. Its Doppler counterpart is the redshifted component, FeSR, which is prominent in the Doppler range of $[1000, 2000]$ km s^{-1} . FeS0 is the second bright region in the Doppler images, and it is prominent in the range of $[-1000, 1000]$ km s^{-1} . The line that indicates this component points straight south (down). The component FeNR is prominent in the Doppler shift range of $[500, 1500]$ km s^{-1} . On one panel in Figure 1, I mark the angles between the lines.

2.2. Molecular maps

Wesson et al. (2026) construct 3D distributions of CO ($J = 2 - 1$) and SiO ($J = 5 - 4$) molecules from ALMA observations of SN 1987A. In Figure 2, I present their CO (upper panels) and SiO (lower panels) intensity maps on the plane of the sky (left panels) and with respect to an observer on the right (right panels), i.e., in a plane along the line of sight. On the left panels, I overlaid the four-line structure that I built in Figure 1, i.e., the lines in the direction of the four outflow components that I identified from the [Fe I] 1.443 μm emission Doppler maps of Larsson et al. (2023). The relative scale of the four lines is 0.67 times that in figure 1. I added the orange arrow in the left panels, which bisects the angle between outflow components FeNR and FeNB.

Figure 2 clearly shows that the molecular gas distribution has a large-scale bipolar structure that is correlated with the Fe outflow components. The bisector between outflow components FeNR and FeNB is along an elongated structure in CO and SiO towards the north-north-east. On the plane of the sky, but not in a plane along the line of sight, it is almost opposite to the component FeSR direction, along which there are clumps of SiO; the angle between the two is 177° . In the SiO map along the line of sight (lower-right panel of Figure 2), the SiO southern clumps are projected on the FeS0 component. In Section 3, I suggest that the southern Fe outflow components and the far south molecular gas are concentrated around the nozzle, a faint radially extended zone in the keyhole (the optical bipolar bright structure) that I attributed to the action of one of the

exploding jets (Soker 2024d). The CO distribution correlated with the general direction of components FeS0 and FeSR. The right panels of Figure 2, in the plane along the line of sight, also reveal the bipolar structure of the molecular gas. I draw two pink arrows at 170° to each other in the SiO map to emphasize this bipolar structure; the CO map also shows it.

Bear & Soker (2018) already hinted at this bipolar structure when referring to the south protrusion in a molecular map from Abellán et al. (2017) as a jet-like feature. On the plane of the sky, it is in the direction of the component FeSR. I present their image between the two lower panels of Figure 2. Bear & Soker (2018) could not fully reveal the molecular gas bipolar structure. The new high-quality images by Wesson et al. (2026) allow the clear identification of the molecular bipolar structure. I will return to discuss this bipolar structure in Section 3.

Wesson et al. (2026) compare their observational finding with numerical simulations of explosions in the framework of the neutrino-driven mechanism. They argue that they can fit the observed CO morphology, but not the SiO velocity distribution and morphology. Specifically, their explosion simulations produce too little Si+O at high velocities, and overpredict the amount of low-velocity material. The JJEM can account for higher-velocity components with energetic jets. The relevant point I make here is that to match the CO morphology, Wesson et al. (2026) examine only the brightest regions of the CO and SiO, i.e., those brighter than twice the noise threshold. In panel (a) of Figure 3, I present the image they compare to one of their simulations. By presenting also the faint regions of the molecular gas, I find the bipolar structure, which I further discuss in Section 3.

To demonstrate the correlation between the molecular morphology and the Fe outflow components, I overlaid a partial transparent intensity map of CO (panel b) and SiO (panel c) from the right panels of Figure 2 on panel (a) of Figure 3. These panels show that the CO and SiO morphologies are correlated, at least in a plane along the line of sight, with the outflow components FeNR, FeNB, and FeS0. The extension of the molecular gas towards FeSR, which is in any case a faint component in [Fe I] 1.443 μm emission, is marginal.

This section shows that the outflow components defined by the [Fe I] 1.443 μm emission and the molecular gas have a correlated bipolar outflow morphology. I turn to compare this with the visible band that exhibits the most prominent bipolar structure, the ‘keyhole.’

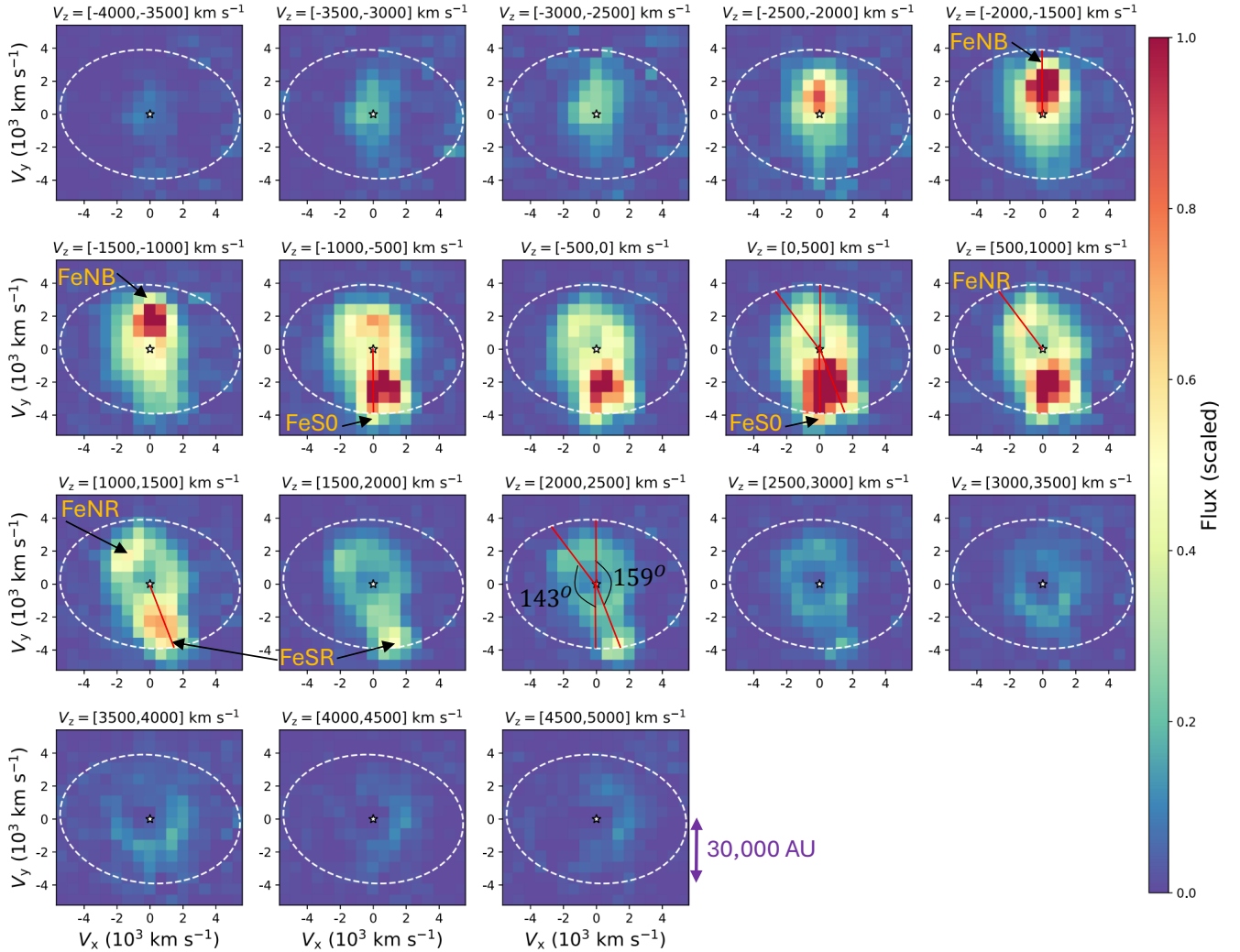


Figure 1. A figure adapted from Larsson et al. (2023), presenting images of the [Fe I] 1.443 μm emission line in Doppler velocity windows, as indicated. The dashed white line shows the position of the equatorial ring that the star lost $\approx 20,000$ yr before explosion. I added the red lines and the names of the outflow components: ‘Fe’ indicates that the components are identified in the [Fe I] 1.443 μm line, ‘N’ and ‘S’ mark north and south, respectively, and the last letter indicates whether the component is blueshifted, redshifted, or has about zero Doppler shift. The observation was on an age of 12,927 days after the explosion; one pixel in the image $0.1'' = 0.024$ pc, corresponds to 664 km s^{-1} in the freely expanding ejecta, for the distance to the LMC of 49.6 kpc that Larsson et al. (2023) assumed.

3. RELATION TO THE BIPOLAR STRUCTURE OF SN 1987A

HST and JWST observations reveal a bipolar structure of a northern low-intensity zone with a bright rim on its front and an elongated low-intensity nozzle in the south; this structure is termed ‘keyhole’.² The morphological similarity of some CCSNRs, including SN 1987A, with the bipolar morphologies of pairs of bubbles

in cooling flow clusters of galaxies (e.g., Soker 2024e) and planetary nebulae (e.g., Soker 2024c), brought me (Soker 2024e) to define the two bubbles and the rim-nozzle asymmetry in SN 1987A, as depicted in Figure 4, and to argue that jets shaped the bipolar structure of SN 1987A (Soker 2024d). Specifically, that one pair of energetic jets was long-lived and shaped the keyhole. Here, I examine the relationship between molecular gas and Fe outflow components and a keyhole’s structure.

On the keyhole image in Figure 4, I overlaid the structure of four red lines and the orange arrow that I constructed in Figure 1 and the left panels of Figure 2:

² See press release by JWST: <https://science.nasa.gov/missions/webb/webb-reveals-new-structures-within-iconic-supernova/>.

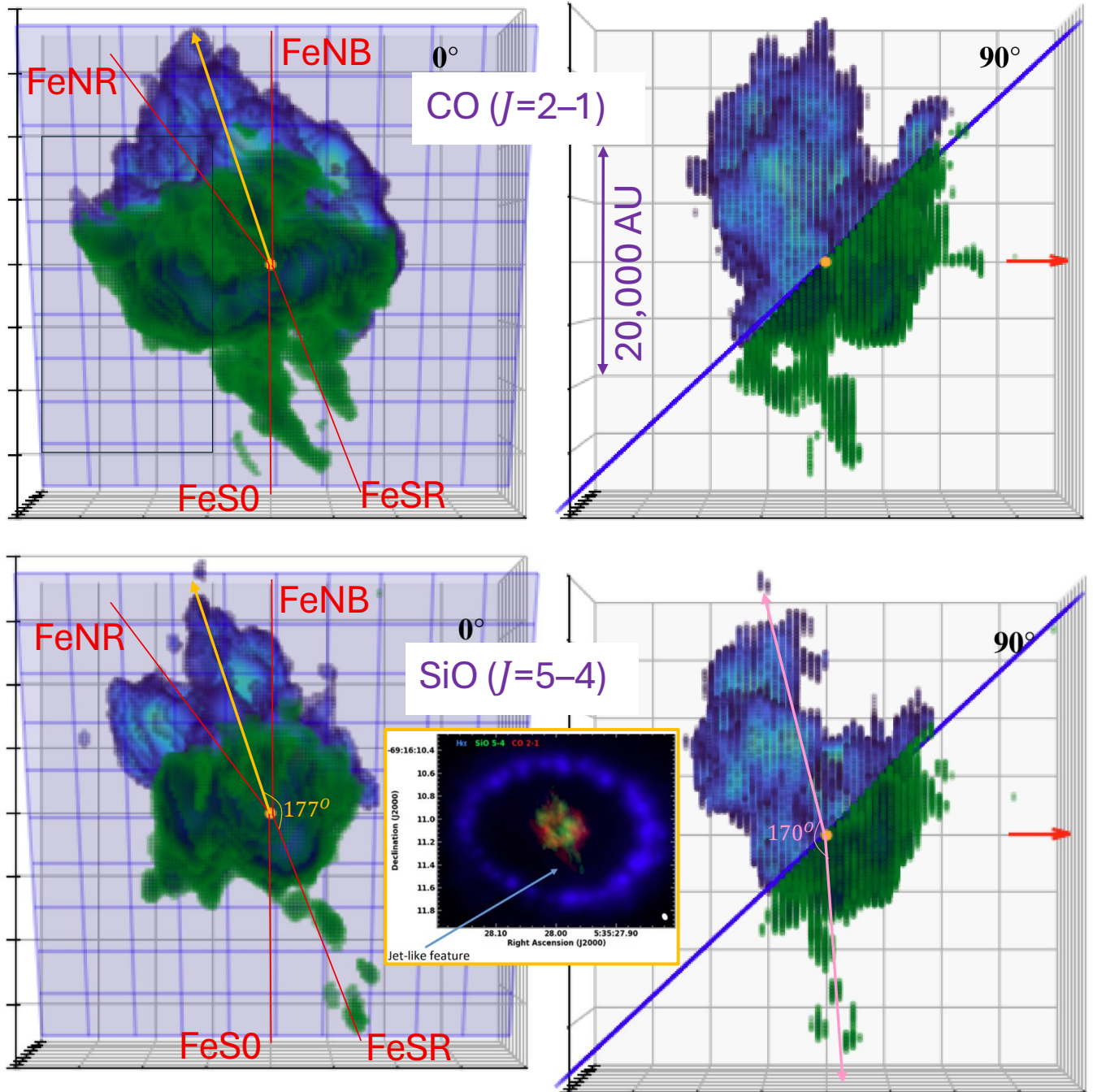


Figure 2. The four large panels are adapted from [Wesson et al. \(2026\)](#). The two upper panels show 3D intensity maps of CO ($J = 2 - 1$) emission, and the two lower panels show 3D intensity maps of SiO ($J = 5 - 4$) emission. The left panel shows the plane of the sky, and in the right panel, Earth is to the right (red arrows point towards Earth). The plane of the equatorial ring is indicated in blue. Blue regions are above the equatorial ring plane, and green material is below it. The orange point marks the explosion's position. Each side of a panel is 40,000 AU. I copied the four-line structures from Figure 1, but the lengths of the lines here are 0.67 times those in Figure 1. I also added the orange arrow in the left panels, which bisects the angle between outflow components FeNR and FeNB, and the two pink arrows in the lower-right panel to emphasize the bipolar structure of the molecular distribution. The inset between the two large lower panels is a figure adapted from [Bear & Soker \(2018\)](#), an image from [Abellán et al. \(2017\)](#) showing CO ($J = 2 - 1$) in red, SiO ($J = 5 - 4$) in red, and H α in blue, i.e., the equatorial ring. The marking of the jet-like feature is from [Bear & Soker \(2018\)](#), who already identified the molecular south outflow.

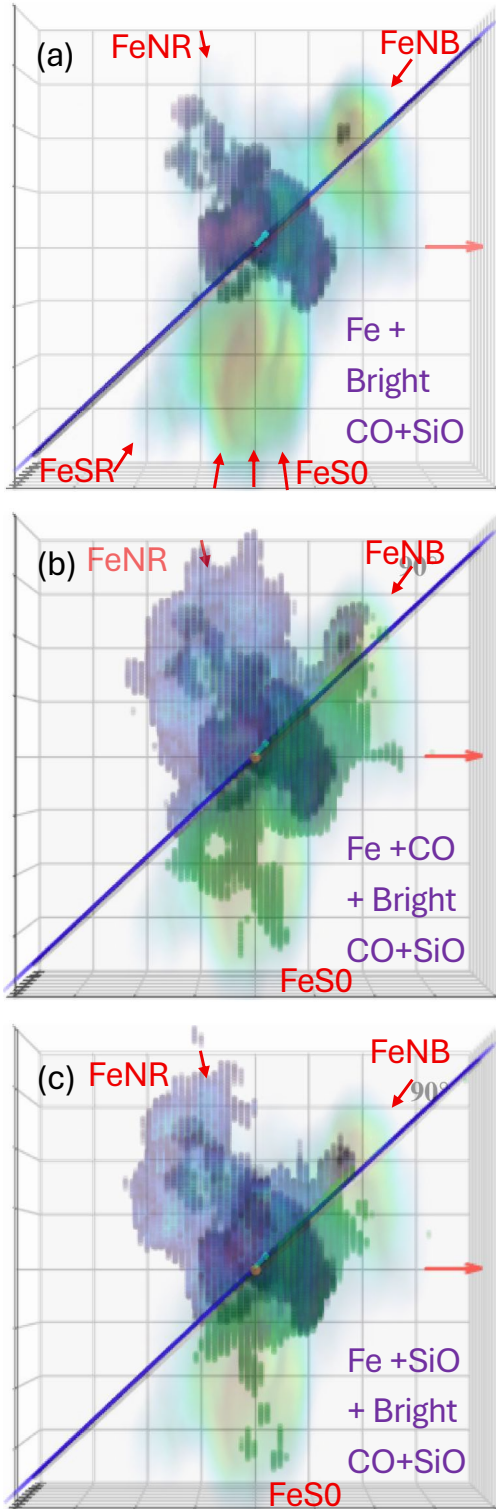


Figure 3. Images adapted from Wesson et al. (2026), with my identification of the four outflow components. (a) Bright CO (dark purple-orange) and SiO (dark purple-green) emission overlaid with the [Fe I] (faint blue to yellow-red) emission that Wesson et al. (2026) obtained from Larsson et al. (2023). Only the regions with intensity above twice the noise threshold are shown by Wesson et al. (2026). (b) A transparent full CO map from Figure 2, which I overlaid on the image from panel (a). (c) A transparent full SiO map from Figure 2, which I overlaid on the image from panel (a).

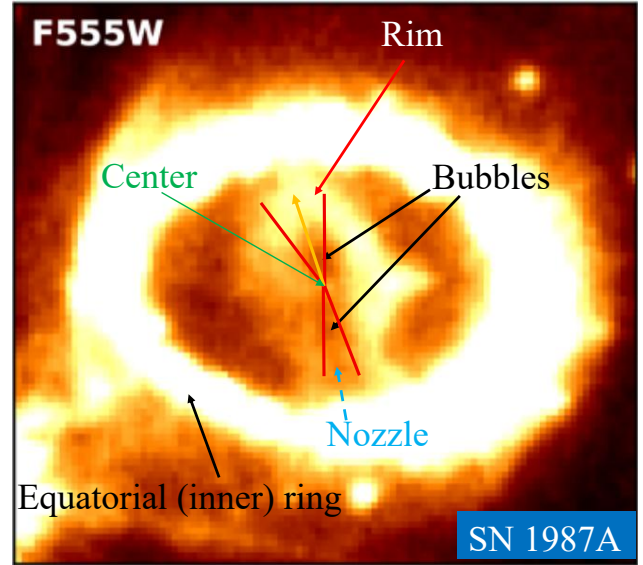


Figure 4. A figure adapted from Soker (2024d) which includes an HST/WFC3 image of SN 1987A in one filter from Rosu et al. (2024); north is up and east to the left. The field of view is $2.50'' \times 2.25''$. The ‘keyhole’ is the north-south elongated bright structure within the equatorial ring. The identification of the rim, nozzle, and two bubbles is from Soker (2024e) based on similarities to jet-inflated bubbles in cooling flow clusters of galaxies. Here I added the structure of the four red lines and the orange arrow from Figure 2, and at the same scale (0.67 times the scale of the four-line structure in Figure 1).

The four red lines depict the Fe outflow components and the orange arrows the bisector of the two north components, which also coincide with the extended molecular gas structure to the north-north-east. In Figure 3, I showed that the molecular gas morphology coincides with three of the Fe outflow components. Figure 4 shows that the bisector between the two northern outflow components is along the bubble and rim in the north, and the two southern outflow components are on the side of the nozzle in the south.

The conclusion of this section is that the Fe outflow components and the extended structure of the molecular gas, namely, the highest velocity components of the molecular gas, are part of the bipolar structure. The southern Fe outflow components are around the nozzle, and the northern ones are around the axis through the center of the northern bubble. The most elongated part of the molecular gas, which is along the orange arrow to the north-north-east (Figure 2), is extended through the bubble and to the front of the rim (the orange arrow in Figure 4). As the earlier papers cited above (Soker 2024e,c) mentioned, the bipolar rim-nozzle asymmetry with two bubbles is a common structure in cooling flow

clusters and planetary nebulae, where it is attributed to shaping by jets. Most likely, a pair of energetic jets shaped the bipolar outflow of SN 1987A (Soker 2024d).

4. DISCUSSION AND SUMMARY

In this short study, I examined the high-quality new analysis of ALMA observations of CO and SiO by Wesson et al. (2026), which I present in Figures 2 and 3. I find a correlation, although not perfect, between the molecular gas structure and the Fe outflow components that I identify in the Doppler maps by Larsson et al. (2023) that I present in Figure 1. Both the molecular gas structure and the Fe outflow components exhibit a general north-south bipolar structure. In Figure 4, I show that the bipolar structure of the [Fe I] 1.443 μm emission outflow components, the fast regions of the molecular gas, and the optical image of SN 1987A, i.e., the keyhole, share the same general bipolar structure. The southern Fe outflow components and the molecular gas are concentrated around the nozzle.

As I discussed in earlier papers (Soker 2024e,d), the keyhole has a morphology similar to that of many jet-shaped pairs of bubbles in cooling-flow clusters of galaxies and planetary nebulae. In Soker (2024c), I argued that the two opposite arcs outside the keyhole appearing in a JWST image by Matsuura et al. (2024), which share the same symmetrical axis as the keyhole, strengthen the claim for shaping by jets. Such arcs are common in jet-shaped bipolar planetary nebulae, and 3D numerical simulations of bipolar jets obtain them (e.g., Akashi et al. 2018).

This study made the bipolar structure more robust, i.e., by emphasizing the nozzle, thereby strengthening the claim that an energetic pair of jets shaped the bipo-

lar structure of SN 1987A. According to the JJEM, this pair was not the only one to participate in the explosion of SN 1987A, but was the most energetic. Other pairs could form more opposite structural features, as I tentatively identified in SN 1987A (Soker 2024b), i.e., a point-symmetric morphology. Point-symmetric morphologies of close to twenty CCSNRs are the most challenging observation for the neutrino-driven mechanism. However, there are others (see reviews cited in Section 1). The next most challenging observational property is the high explosion energies of some CCSNe that are way above the reach of the energies that simulations of the neutrino-driven mechanism can obtain of $E_{\text{exp}} \simeq 2 \times 10^{51}$ erg. For example, three out of six CCSNe studied by Zhao et al. (2026) are beyond the reach of the neutrino-driven mechanism. Adding a powerful magnetar will not help much, as such magnetars require a jet-driven explosion (e.g., Soker & Gilkis 2017; Kumar 2025).

This study provides support for the claim that the JJEM is the primary explosion mechanism in CCSNe. Other energy sources can boost the jet-driven explosion (e.g., Soker 2026b), including neutrino heating (Soker 2022), a magnetar (e.g., Soker & Gilkis 2017), and, in rare cases, thermonuclear burning triggered by the collapse of a pre-collapse mixed layer of helium and oxygen (Klimov et al. 2026, in preparation; for the thermonuclear process itself see, e.g., Kushnir & Katz 2015; Blum & Kushnir 2016).

ACKNOWLEDGMENTS

A grant from the Pazy Foundation 2026 supported this research. I thank the Charles Wolfson Academic Chair at the Technion.

REFERENCES

- Abellán, F. J., Indebetouw, R., Marcaide, J. M., et al. 2017, *ApJL*, 842, L24, doi: [10.3847/2041-8213/aa784c](https://doi.org/10.3847/2041-8213/aa784c)
- Akashi, M., Bear, E., & Soker, N. 2018, *MNRAS*, 475, 4794, doi: [10.1093/mnras/sty029](https://doi.org/10.1093/mnras/sty029)
- Alp, D., Larsson, J., Maeda, K., et al. 2019, *ApJ*, 882, 22, doi: [10.3847/1538-4357/ab3395](https://doi.org/10.3847/1538-4357/ab3395)
- Bear, E., & Soker, N. 2018, *MNRAS*, 478, 682, doi: [10.1093/mnras/sty1053](https://doi.org/10.1093/mnras/sty1053)
- Blum, K., & Kushnir, D. 2016, *ApJ*, 828, 31, doi: [10.3847/0004-637X/828/1/31](https://doi.org/10.3847/0004-637X/828/1/31)
- Bouchet, P., Gastaud, R., Coulais, A., et al. 2024, *ApJ*, 965, 51, doi: [10.3847/1538-4357/ad2770](https://doi.org/10.3847/1538-4357/ad2770)
- Gabler, M., Wongwathanarat, A., & Janka, H.-T. 2021, *MNRAS*, 502, 3264, doi: [10.1093/mnras/stab116](https://doi.org/10.1093/mnras/stab116)
- Giudici, B., Gabler, M., & Janka, H.-T. 2025, arXiv e-prints, arXiv:2511.11796, <https://arxiv.org/abs/2511.11796>
- Janka, H.-T. 2025a, *Annual Review of Nuclear and Particle Science*, 75, 425, doi: [10.1146/annurev-nucl-121423-100945](https://doi.org/10.1146/annurev-nucl-121423-100945)
- Janka, H.-T., Gabler, M., & Wongwathanarat, A. 2017, in *IAU Symposium*, Vol. 331, *Supernova 1987A:30 years later - Cosmic Rays and Nuclei from Supernovae and their Aftermaths*, ed. A. Marcowith, M. Renaud, G. Dubner, A. Ray, & A. Bykov, 148–156, doi: [10.1017/S1743921317004549](https://doi.org/10.1017/S1743921317004549)
- Janka, T. 2025b, *Video Memorie della Societa Astronomica Italiana*, 2, 46, doi: [10.36116/VIDEOMEM.2.2025.46](https://doi.org/10.36116/VIDEOMEM.2.2025.46)

- Jerkstrand, A., Wongwathanarat, A., Janka, H.-T., et al. 2020, *MNRAS*, 494, 2471, doi: [10.1093/mnras/staa736](https://doi.org/10.1093/mnras/staa736)
- Kumar, A. 2025, *NewA*, 116, 102346, doi: [10.1016/j.newast.2024.102346](https://doi.org/10.1016/j.newast.2024.102346)
- Kushnir, D., & Katz, B. 2015, *ApJ*, 811, 97, doi: [10.1088/0004-637X/811/2/97](https://doi.org/10.1088/0004-637X/811/2/97)
- Larsson, J., Fransson, C., Spyromilio, J., et al. 2016, *ApJ*, 833, 147, doi: [10.3847/1538-4357/833/2/147](https://doi.org/10.3847/1538-4357/833/2/147)
- Larsson, J., Fransson, C., Sargent, B., et al. 2023, *ApJL*, 949, L27, doi: [10.3847/2041-8213/acd555](https://doi.org/10.3847/2041-8213/acd555)
- Luo, Y., Zha, S., & Kajino, T. 2026, *PhRvD*, 113, 023024, doi: [10.1103/PhysRevD.113.023024](https://doi.org/10.1103/PhysRevD.113.023024)
- Matsuura, M., Boyer, M., Arendt, R. G., et al. 2024, *MNRAS*, 532, 3625, doi: [10.1093/mnras/stae1032](https://doi.org/10.1093/mnras/stae1032)
- McCray, R., & Fransson, C. 2016, *ARA&A*, 54, 19, doi: [10.1146/annurev-astro-082615-105405](https://doi.org/10.1146/annurev-astro-082615-105405)
- Murphy, R. D., Brinkman, E., Richardson, C. J., et al. 2025, arXiv e-prints, arXiv:2511.21895, doi: [10.48550/arXiv.2511.21895](https://doi.org/10.48550/arXiv.2511.21895)
- Ono, M., Nagataki, S., Ferrand, G., et al. 2020, *ApJ*, 888, 111, doi: [10.3847/1538-4357/ab5dba](https://doi.org/10.3847/1538-4357/ab5dba)
- Orlando, S. 2026, arXiv e-prints, arXiv:2601.17499, doi: [10.48550/arXiv.2601.17499](https://doi.org/10.48550/arXiv.2601.17499)
- Orlando, S., Ono, M., Nagataki, S., et al. 2020, *A&A*, 636, A22, doi: [10.1051/0004-6361/201936718](https://doi.org/10.1051/0004-6361/201936718)
- Orlando, S., Miceli, M., Ono, M., et al. 2025, *A&A*, 699, A305, doi: [10.1051/0004-6361/202554862](https://doi.org/10.1051/0004-6361/202554862)
- Rosu, S., Larsson, J., Fransson, C., et al. 2024, *ApJ*, 966, 238, doi: [10.3847/1538-4357/ad36cc](https://doi.org/10.3847/1538-4357/ad36cc)
- Rusakov, A., Burrows, A. S., Wang, T., & Vartanyan, D. 2026, arXiv e-prints, arXiv:2602.09025, <https://arxiv.org/abs/2602.09025>
- Shiran, K., & Soker, N. 2025, arXiv e-prints, arXiv:2512.16554, doi: [10.48550/arXiv.2512.16554](https://doi.org/10.48550/arXiv.2512.16554)
- Soker, N. 2017, *Research in Astronomy and Astrophysics*, 17, 113, doi: [10.1088/1674-4527/17/11/113](https://doi.org/10.1088/1674-4527/17/11/113)
- . 2022, *Research in Astronomy and Astrophysics*, 22, 095007, doi: [10.1088/1674-4527/ac7cbc](https://doi.org/10.1088/1674-4527/ac7cbc)
- . 2024a, *Universe*, 10, 458, doi: [10.3390/universe10120458](https://doi.org/10.3390/universe10120458)
- . 2024b, *NewA*, 107, 102154, doi: [10.1016/j.newast.2023.102154](https://doi.org/10.1016/j.newast.2023.102154)
- . 2024c, *Galaxies*, 12, 29, doi: [10.3390/galaxies12030029](https://doi.org/10.3390/galaxies12030029)
- . 2024d, *Research in Astronomy and Astrophysics*, 24, 075006, doi: [10.1088/1674-4527/ad4fc2](https://doi.org/10.1088/1674-4527/ad4fc2)
- . 2024e, *The Open Journal of Astrophysics*, 7, 49, doi: [10.33232/001c.120279](https://doi.org/10.33232/001c.120279)
- . 2025a, *NewA*, 121, 102453, doi: [10.1016/j.newast.2025.102453](https://doi.org/10.1016/j.newast.2025.102453)
- . 2025b, arXiv e-prints, arXiv:2509.19264, doi: [10.48550/arXiv.2509.19264](https://doi.org/10.48550/arXiv.2509.19264)
- . 2026a, arXiv e-prints, arXiv:2602.09993, doi: [10.48550/arXiv.2602.09993](https://doi.org/10.48550/arXiv.2602.09993)
- . 2026b, arXiv e-prints, arXiv:2511.14578, doi: [10.48550/arXiv.2511.14578](https://doi.org/10.48550/arXiv.2511.14578)
- Soker, N., & Gilkis, A. 2017, *ApJ*, 851, 95, doi: [10.3847/1538-4357/aa9c83](https://doi.org/10.3847/1538-4357/aa9c83)
- Utrobin, V. P., Wongwathanarat, A., Janka, H.-T., & Müller, E. 2015, *A&A*, 581, A40, doi: [10.1051/0004-6361/201425513](https://doi.org/10.1051/0004-6361/201425513)
- Varma, V., & Müller, B. 2026, arXiv e-prints, arXiv:2601.18357, doi: [10.48550/arXiv.2601.18357](https://doi.org/10.48550/arXiv.2601.18357)
- Wang, N. Y. N., Shishkin, D., & Soker, N. 2025, arXiv e-prints, arXiv:2510.02203, doi: [10.48550/arXiv.2510.02203](https://doi.org/10.48550/arXiv.2510.02203)
- Wesson, R., Gabler, M., Lyons, M., et al. 2026, arXiv e-prints, arXiv:2602.11259, doi: [10.48550/arXiv.2602.11259](https://doi.org/10.48550/arXiv.2602.11259)
- Wongwathanarat, A., Müller, E., & Janka, H. T. 2015, *A&A*, 577, A48, doi: [10.1051/0004-6361/201425025](https://doi.org/10.1051/0004-6361/201425025)
- Zhao, J., Jiang, J.-a., Xu, Z., et al. 2026, arXiv e-prints, arXiv:2602.17275, doi: [10.48550/arXiv.2602.17275](https://doi.org/10.48550/arXiv.2602.17275)